A New Multifunctional Ferrocenyl-Substituted Ferrocenophane Derivative: Optical and Electronic Properties and Selective Recognition of Mg^{2+} Ions

Juan Luis Lopez,[a] Alberto Tárraga,[a] Arturo Espinosa,[a] M. Desamparados Velasco,[a] Pedro Molina,*[a] Vega Lloveras,[b] José Vidal-Gancedo,[b] Concepció Rovira,[b] Jaume Veciana,*[b] David J. Evans,[c] and K. Wurst[d]

Abstract: The synthesis, characterisation, and X-ray structure of a new strained asymmetric diferrocene derivative (**2**) is reported. Compound **2** acts as a highly specific electrochemical and optical Mg^{2+} ion sensor, as revealed by spectroscopic and electrochemical techniques. Thus, in the presence of Mg^{2+}, a new redox peak appears in the cyclic voltammogram (CV) that is anodically shifted compared to the $E_{1/2}$ of the free receptor ($\Delta E_{1/2} = 340$ mV). Diferrocene derivative **2** also gives a highly visual response upon addition of Mg^{2+}, namely a change of colour from orange to deep purple. In addition, compound **2** does not show any significant sensing activity in the presence of Ca^{2+} or alkaline ions. On protonation, it is converted into the stable diferrocenylcarbenium salt **4**, in which two different modes of stabilisation of the α-carbocationic centre are clearly demonstrated by a combination of ^{1}H NMR and ^{57}Fe Mössbauer spectroscopic measurements. Finally, by a partial (chemical or electrochemical) oxidation, compound **2** forms the asymmetric mixed-valence species $\mathbf{2}^{+}$, which can be isolated as the solid salt **6** by using $CF_3SO_3^-$ as a counterion. This mixed-valence species shows a fast intramolecular electron-transfer process, as ascertained by several spectroscopic techniques.

Keywords: electrochemistry · electron transfer · metallocenes · molecular recognition · Mössbauer spectroscopy

Introduction

The chemistry of ferrocene-based structures has been receiving increasing attention because of their importance in many fields such as electrochemistry, molecular recognition, material science and catalysis.[1] We have focussed our attention on two important aspects of the chemistry of these materials, namely molecular recognition and intramolecular electron transfer in mixed-valence diferrocene derivatives.

Design of redox-active receptors in which a change in electrochemical behaviour can be used to monitor complexation of guest species is an increasingly important area of molecular recognition.[2] In this context, ferrocene derivatives, mostly those which are substituted with macrocyclic ligands, are prototype molecules which have proved to be especially versatile as ion sensors.[3] Cation binding at an adjacent receptor site of a ferrocene-based host induces a positive shift in the redox potential of the ferrocene/ferrocenium couple, either by through-bond and/or through-space electrostatic interactions, interference or conformational change,[4] and the complexing ability of the ligand can be reversibly switched on or off by varying the applied electrochemical potential. The efficiency of these kinds of redox-active ligands crucially depends on the electronic communication between the metal centre involved. It has been shown that this communication is very favourable when donor atoms of a chelating ligand are directly attached to the ferrocene units.[3e,5] In particular, it has been suggested that an added degree of recognition is conferred by appearance of a new set of redox waves (two-wave behaviour) as-

[a] J. L. Lopez, Dr. A. Tárraga, Dr. A. Espinosa, Dr. M. D. Velasco, Prof. P. Molina
Universidad de Murcia
Departamento de Química Orgánica
Facultad de Química, Campus de Espinardo
30100 Murcia (Spain)
Fax: (+34) 968-364-149
E-mail: pmolina@um.es

[b] V. Lloveras, Dr. J. Vidal-Gancedo, Prof. C. Rovira, Prof. J. Veciana
Institut de Ciencia de Materials de Barcelona (CSIC)
Campus Universitari de Bellaterra, 08193 Cerdanyola (Spain)
Fax: (+34) 93-580-5729
E-mail: vecianaj@icmab.es

[c] Dr. D. J. Evans
Department of Biological Chemistry, John Innes Centre
Norwich Research Park, Colney, Norwich, NR4 7UH (UK)

[d] Dr. K. Wurst
Institut für Allgemeine Anorganische und Theoretische Chemie
Universität Innsbrück, 6020, Innarain 52a, Innsbrück (Austria)

Supporting information for this article is available on the WWW under http://www.chemeurj.org/ or from the author.

 DOI: 10.1002/chem.200305394

sociated with the oxidation of the ferrocene unit in the host–guest complex, compared with a single gradual shift in the potential of the original ferrocene redox couple.[6]

Since the advent of mixed-valence chemistry in 1967,[7] the study of electronic interactions in systems containing multiple, identical metal-centred fragments that individually display fast, reversible, one-electron exchange has been a topic of particular interest.[8] Mixed-valence compounds, which have at least two redox sites in different oxidation states linked by a bridge that mediates the transfer of electrons from one site to the other, are excellent benchmarks for the study of intramolecular electron-transfer phenomena.[9] In this context, many complexes containing two ferrocenyl moieties, which are linked together with a wide variety of structural motifs, have been synthesised to investigate the effectiveness of the bridging groups for electron transfer between the redox nuclei. Variation of the nature of the molecular framework of the bridge enables the extent of communication between the metal centres to be modulated, as reflected by the electrochemical response. Full characterisation of this kind of interaction between two iron atoms is provided by the electronic coupling parameter (V_{ab}), which has the units of energy and can be obtained from the position, intensity and width of the intervalence transition band, which generally occurs in the near infrared region.[10,11] Although metal–metal interactions of differing extents have been revealed for homobimetallic complexes in which the two ferrocene units are coupled intimately by π-unsaturated bridges,[12] heterocycles[13] or metallocycles,[14] examples that show electronic coupling between ferrocenyl units either through a carbenium ion[15] or hydroxyl-substituted sp^3 carbon atoms[16] are rare.

As shown in Figure 1, the structural features required for the properties of particular interest to us in ferrocene chemistry are very different: an effective spacer is needed to observe the intramolecular electron-transfer phenomena in diferrocene compounds, whereas the presence of an heteromacrocycle is the structural motif that is almost mandatory for molecular recognition processes.

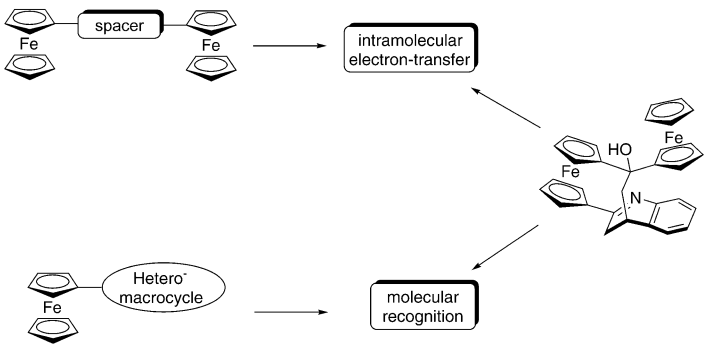

Figure 1. Schematic diagram of the structural features required for intramolecular electron-transfer phenomena and molecular recognition processes.

This paper is devoted to the preparation, structural determination and study of the physicochemical properties of the new diferrocene derivative **2**. This compound exhibits a defined topology with a ferrocenophane architecture and also incorporates an aza-substituted bridge. The combined effects of both structural characteristics suggest that: 1) it might experience an electron-cloud perturbation upon coordination or protonation and may thus function as a chemosensor for metal ions or protons; and 2) it could be converted by partial oxidation (chemical or electrochemical) into the corresponding mixed-valence compound $\mathbf{2}^+$, which would display interesting intramolecular electron-transfer phenomena and show coordination properties that should differ from those of the neutral derivative. Consequently, the combination of these two properties in diferrocene **2** could lead to interesting properties, such as electrochemically switchable chemosensing behaviour.

Results and Discussion

Diferrocenylcarbinol 2

Synthesis: This compound was prepared from the ferrocenophane **1**,[17] which can be viewed either as a [5]ferrocenophane bearing a 2,4-bridged dihydroquinoline ring or as a [4](2,4)-dihydroquinolinophane containing a 1,1′-disubstituted ferrocene bridge. Reaction of ferrocenophane **1** with ferrocenyllithium[18] in dry THF at room temperature under N_2 provided, after chromatographic purification, the diferrocenylcarbinol **2** as an orange solid, in 80% yield. (Scheme 1).

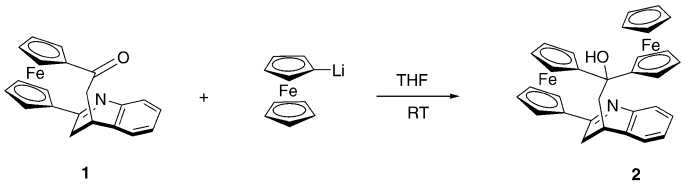

Scheme 1. Reaction scheme for the formation of compound **2**.

X-ray structure determination: Single crystals of **2** suitable for X-ray structure determination were grown from CH_2Cl_2/hexane. The molecular structure is shown in Figure 2 together with the numbering scheme. Compound **2** crystallises in the monoclinic space group $P2_1/n$ with four molecules in the unit cell. The molecular structure of **2** reveals almost eclipsed cyclopentadienyl rings for both ferrocenes. The differences between both ferrocenes are observed in the Fe–C(cyclopentadienyl) distances. Thus, whereas in the monosubstituted ferrocene the Fe–C distances are between 2.025 and 2.051 Å, in the disubstituted ferrocene the distances range between 2.024 and 2.084 Å. This generates a deformation angle between the two ring centroids and the iron atom of 176.5° for the monosubstituted and 175.6° for the disubstituted ferrocene, and tilt angles between the planes of the Cp rings of 3.5° and 5.8°, respectively. The deformation angle of the unstrained monosubstituted ferrocene can accrue from crystal packing effects. More evidence for the conformational strain is the bending of the single bonds C(20)–C(21) and C(10)–C(21) with respect to the Cp rings. Atom C(21) lies 0.021 Å and 0.277 Å out of the Cp planes

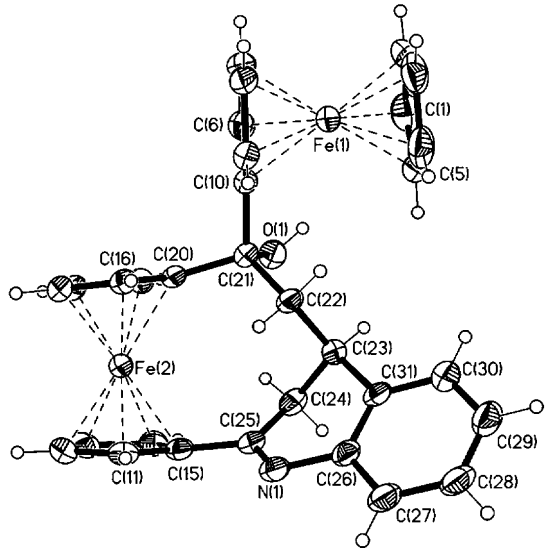

Figure 2. ORTEP view of the molecular structure of compound **2** showing the atom labelling in the asymmetric unit. Thermal ellipsoids are drawn at 50% probability level.

of the mono- and disubstituted ferrocene, respectively. The single bonds C(10)–C(21) and C(20)–C(21) have bending angles of 0.8° and 10.5°, respectively, in the opposite direction of the iron atoms. Interestingly, the bending angle of the single bond C(15)–C(25) is 5.6° in the direction of the iron atom of the disubstituted ferrocene. This bending in the direction of the iron atom can often be found in monosubsituted ferrocenes with aldehyde groups or vinyl groups with electron-withdrawing substituents, which can conjugate with the Cp ring. In these compounds the bending angles are in a range between 2° and 4°. The strain observed in the disubstituted ferrocene is, as expected, much smaller than that found in a related 2-aza[3]ferrocenophane compound, which has the nitrogen atom linked to both bridge carbons of the ferrocene, thus enforcing a rigid bridge geometry.[17b] In contrast to that compound, which has a short Fe–N distance, in **2** the nitrogen atom is far from the Fe atom of the disubstituted ferrocene, as it is situated in the external part of the molecule and, therefore, close interaction of the nitrogen atom with the iron atoms of each ferrocene unit is prevented. The monosubstituted ferrocene unit has a short Fe–HO interaction (d_{Fe-HO} 2.989 Å) reminiscent of agostic type bonding. The two ferrocene units are almost orthogonal, forming an angle of 106.93° between the closest Cp rings. On the other hand, only a small torsion angle is observed between the Cp ring of the disubstituted ferrocene and the aromatic ring connected to the nitrogen atom, thus promoting an available resonance pathway.

Table 1. ^{1}H NMR data for the three substituted Cp rings in compounds **2** and **4**.

	Compound	δH_2	δH_3	δH_4	δH_5	$\Delta\delta H_{2,3}$	$\Delta\delta H_{5,4}$
2	Cp_1	3.88	3.99	4.07	3.96	0.11	−0.11
	Cp_2	4.72	4.53	4.45	4.99	−0.19	−0.46
	Cp_3	4.41	4.14	4.14	3.80	−0.27	0.34
4	Cp_1	5.05	4.91	5.27	6.10	−0.14	−0.83
	Cp_2	5.86	5.51	5.12	5.66	−0.35	−0.54
	Cp_3	5.53	6.63	6.67	5.88	1.10	0.79

^{1}H NMR studies: An in-depth study of the ^{1}H NMR spectrum of the diferrocenylcarbinol **2** has been carried out. The room temperature 400 MHz ^{1}H NMR spectra of **2** was completely assigned (with the exception of the aromatic protons) by ^{1}H,^{1}H COSY, NOESY and spin-decoupled experiments. The analysis of its ^{1}H NMR spectrum presents the following characteristic features: 1) the diastereotopism of all the protons within the three substituted Cp rings, which appear as twelve multiplets in contrast to the singlet corresponding to the five equivalent protons within the unsubstituted Cp_4 ring (Table 1); 2) the diastereotopism shown by the two protons within each of the two methylene groups of the bridge, which appear at $\delta = 1.99$ ppm (t) and 2.41 ppm (dd), in the case of the CH_2 group placed at the 2-position of the bridge, and at $\delta = 2.52$ ppm (dd) and 3.70 ppm (dd), in the case of the CH_2 group placed in the dihydroquinoline moiety; 3) the methine group which appears as a multiplet at $\delta = 3.38$ ppm and iv) the OH group, which appears as a singlet at $\delta = 2.57$ ppm.

The results obtained from NOE experiments are illustrated in Figure 3. It is important to emphasise that while a NOE effect is detected between the OH group and the hydrogen atom H2 present in Cp_3, no effect is observed between the OH group and the hydrogen atom H5 within the same Cp_3 ring. This indicates that, although in principle a free rotation around the C_{OH}–C_{Cp3} bond could be assumed, giving rise to two possible extreme rotamers, from the NOE experiments only the rotamer shown in Figure 3 is detected. Moreover, inspection of the X-ray structure of alcohol **2** reveals the occurrence of an Fe···HO interaction ($d_{Fe\cdots H}$: 2.989 Å), reminiscent of the agostic type bonding reported for the protonation product of ferrocene and its proton exchange in highly acidic media,[19] and the intermediates in electrophilic substitution reactions on ferrocenes.[20] The interaction could account, to some extent, for a hampered rotation of the monosubstituted ferrocene unit.

Electrochemical study: An electrochemical study in CH_2Cl_2 was carried out at room temperature, with $[NnBu_4]ClO_4$ (0.1 M) as supporting electrolyte, a Pt disk as a working electrode and SCE as the reference electrode. The cyclic voltammetric (CV) response of **2** shows two closely spaced reversible oxidation processes at +0.510 V and +0.740 V (vs SCE electrode in CH_2Cl_2) (Table 2 and Figure 4). Likewise the differential pulse voltammogram (DPV) also exhibits two well-resolved oxidation waves of the same area.[21] The first reversible oxidation process arises from the oxidation of the monosubstituted ferrocene unit, while the second reversible oxidation process is associated with the oxidation of the 1,1′-disubstituted ferrocene unit. One might speculate

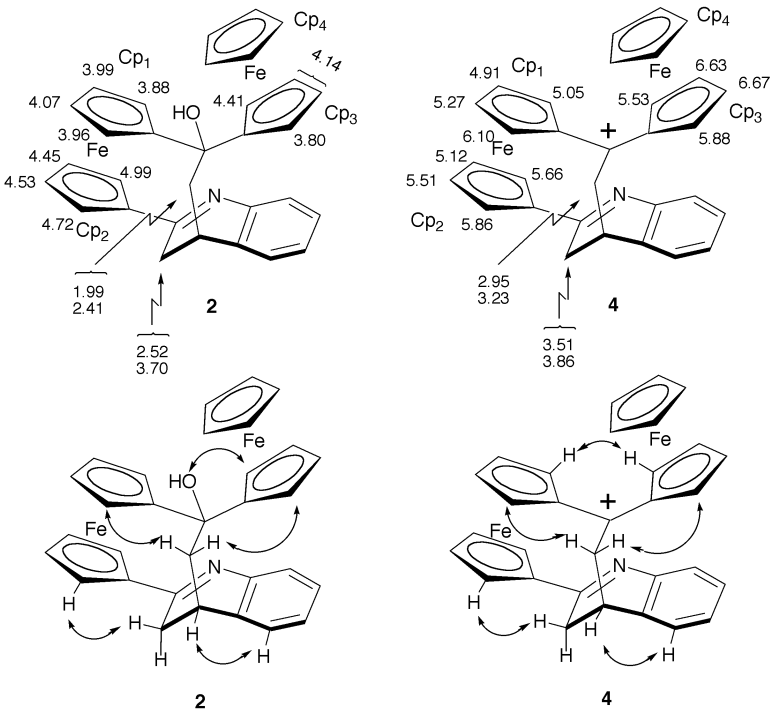

Figure 3. Chemical shifts and NOEs observed for compounds **2** and **4**.

Table 2. Cyclic voltammetry data.

	$E_{1/2}$ (1)[a] ($E_{pa}-E_{pc}$)		$E_{1/2}$ (2)[a] ($E_{pa}-E_{pc}$)		$E_{1/2}$ (3)[a] ($E_{pa}-E_{pc}$)	E_{pc} (irrev) (1)		E_{pc} (irrev) (2)	
	CH_3CN	CH_2Cl_2	CH_3CN	CH_2Cl_2	CH_3CN	CH_3CN	CH_2Cl_2	CH_3CN	CH_2Cl_2
2	0.450 (0.070)	0.510 (0.070)	0.670 (0.080)	0.740 (0.080)					
2·Mg^{2+}[b]	0.570 (0.080)		0.760 (0.070)		1.100 (0.070)	−0.430			
3	0.480 (0.060)	0.540 (0.080)	1.020 (0.070)	1.060 (0.140)		broad wave	−0.560		
4			0.985 (0.095)	1.160 (0.140)		−0.130	−0.070	−0.310	−0.260
6	0.470 (0.070)		1.010 (0.080)			−0.450			

[a] $E_{1/2}=(E_{pa}+E_{pc})/2$ versus SCE in volts. Electrolyte: [N*n*Bu$_4$]ClO_4; working and counter electrodes: Pt; reference electrode: SCE. [b] $E_{1/2}=(E_{pa}+E_{pc})/2$ versus decamethylferrocene (internal reference), in volts. Data obtained from measurements in CH_3CN/CH_2Cl_2 (3:2) as solvent. Under these conditions the redox potentials of compound **2** were: $E_{1/2}(1)=+0.540$ V and $E_{1/2}(2)=+0.760$ V versus DMFc.

that the difference between the oxidation waves ($\Delta E_{1/2}=$ 230 mV) in compound **2**, as well as the fact that the second oxidation process appears at a higher potential than those observed for closely related ferrocenophanes[17b] (0.740 V vs 0.580 V), is direct evidence for the presence of electronic communication between the two ferrocene units. However, we hesitate to invoke this explanation, because, even in the absence of communication, the difference between the potentials will increase simply because of the electrostatic effect.[22] In addition, the two ferrocenyl groups are intrinsically inequivalent and this also contributes to the difference in the oxidation potentials of the two ferrocene moieties. At this time, with only the electrochemical data, it is not possible to separate the combined effects of, or to determine the relative contribution of, chemical inequivalence and electronic communication through the carbon chain.

Metal-ion sensing properties of **2**: One of the most interesting attributes of compound **2** is the presence of two ferrocene redox-active moieties in proximity to the cation-binding dihydroquinoline site. The metal-recognition properties of proligand **2** were therefore evaluated by CV.[23] Whereas no perturbation of the CV was observed upon addition of Ca^{2+} ion, significant modification could be observed upon addition of Mg^{2+} ion. Thus, on addition of $Mg(ClO_4)_2$, a clear evolution of the second wave from $E_{1/2}=0.760$ V to 1.100 V ($\Delta E_{1/2}=340$ mV) was observed, whereas there was almost no effect on the first wave (a change from $E_{1/2}=0.540$ V to 0.570 V ($\Delta E_{1/2}=30$ mV)). More interesting is the observation of an extra irreversible reduction wave at $E_{1/2}=-0.430$ V, which is absent for the proligand. The current intensity of the anodic peak of the newly appearing reversible wave increases, while that of the disappearing reversible wave diminishes, with a linear dependence on the number of equivalents of the salt added; maximum perturbation of the CV was obtained with one equivalent of added Mg^{2+} ion (Table 2 and Figure 4). This "two-wave" behaviour is diagnostic of a large value for the equilibrium constant for cation binding by the neutral receptor.[6] The binding enhancement factor (BEF) is 1.8×10^{-6} and the reaction coupling efficiency[2d,e] (RCE) is 5.5×10^{5}. Remarkably, the presence of alkaline metal ions in solution ($LiClO_4$, $NaClO_4$ and $KClO_4$) had no effect on the CV, even when present in large excess. The major challenge in the design of Mg^{2+} sensors lie, for many applications, in the discrimination of Mg^{2+} ions from Ca^{2+}, Na^+ and K^+, as they play important roles as intracellular messengers in the regulation of cell function.[24] In this context, a number of redox-active ferrocene-based receptors such as imine-,[25] oxazoline-,[26] imidazoline-,[27] and pyridine-functionalised[28] ferrocene ligands have been described, which, in organic solvents, selectively respond to, but do not clearly

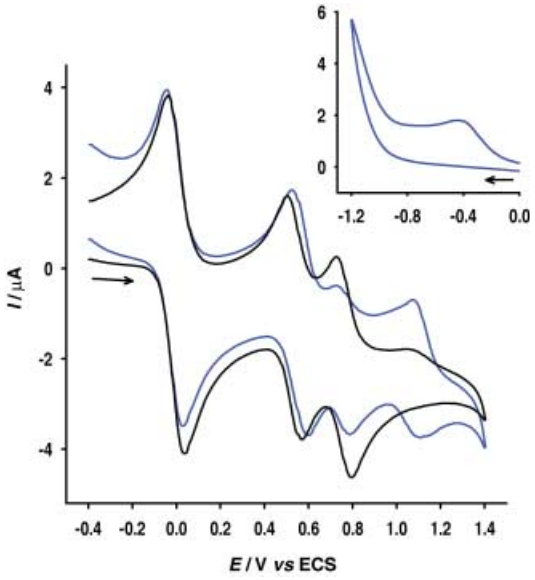

Figure 4. Cyclic voltammogram of compound **2** before (black) and after addition of 1 equivalent of $Mg(ClO_4)_2$ (blue); 1 mM **2** and 0.1 M $[NnBu_4]ClO_4$ in CH_3CN/CH_2Cl_2 also containing 1 mM DMFc, scan rate: 0.2 $V s^{-1}$. The average of anodic and cathodic peak potentials $(E_{pa}+E_{pc})/2$ for DMFc was set at 0 V in each voltammogram.

Table 3. UV-visible/near-IR data in CH_2Cl_2.

Compound	λ_{max} [nm] (10^3 ε [$M^{-1}cm^{-1}$])
2	319 (8.2), 464 (1.2)
2·Mg^{2+}	530 (4.6)
3	342 (10.2), 530 (3.5), 731 (0.2)
4	325 (14.7), 375 (h), 465 (3.9), 641 (3.1)
6	329 (10.0), 507 (1.4), 625 (sh), 1230 (0.03)
$\mathbf{2}^{+1}$[a]	330 (10.5), 520[b] (1.8), 630 (sh), 1240 (0.03)
$\mathbf{2}^{+2}$[a]	339 (12.8), 524 (2.8), 630 (sh).

[a] Oxidised species obtained electrochemically in CH_2Cl_2 with 0.15 M nBu_4NPF_6. [b] Value obtained by deconvolution of the experimental spectrum.

differentiate between, Mg^{2+} and Ca^{2+} ions, with no interference from large excesses of Li^+, Na^+ and K^+.

We have discounted the possibility that the electrochemical response we observed upon addition of Mg^{2+} ion is due to adventitious protonation or hydration of the ligand. Addition of water to the resultant electrochemical solution elicited a further redox response, with the evolution of a new redox wave that corresponds to that assigned to the proligand. Therefore it can be concluded that metal-ion coordination occurs. The proligand **2** can be recovered unchanged in almost quantitative yield by aqueous workup.

The large positive shift in the ferrocene redox potential, upon coordination of Mg^{2+} ions by **2**, prompted us to investigate whether the coordination has an effect on the UV/Vis spectrum, as previous studies on ferrocene-based ligands have shown that their characteristic low-energy bands (LE) are perturbed by complexation.[29]

The UV-visible spectrum of **2** is consistent with most ferrocenyl chromophores in that they exhibit two charge-transfer bands in the visible region.[30] The prominent band at 319 nm ($\varepsilon = 8240\ M^{-1}cm^{-1}$; high energy (HE)), is assigned to a ligand-centred π–π* electronic transition (L–π*), and the less energetic and weaker band at 464 nm ($\varepsilon = 1195\ M^{-1}cm^{-1}$) (LE), responsible for the bright orange colour of this compound, is attributed to a metal-to-ligand charge-transfer (MLCT) process (d_π–π*) (Table 3). This assignment is in accordance with the latest theoretical treatment (model III) reported by Barlow et al.[31] The bands associated with the d–d transitions are masked by the MLCT band.[32]

Addition of anhydrous $Mg(ClO_4)_2$ into a solution of **2** in dichloromethane caused a progressive appearance of a new, more intense, absorption band located at $\lambda = 530$ nm ($\varepsilon = 4580\ M^{-1}cm^{-1}$) and the complete disappearance of the initial LE band (Figure 5). The new band, which is 76 nm red-shifted, is assigned to MLCT (d_π–π*) transitions in the complexed ligand and is responsible for a change of colour from

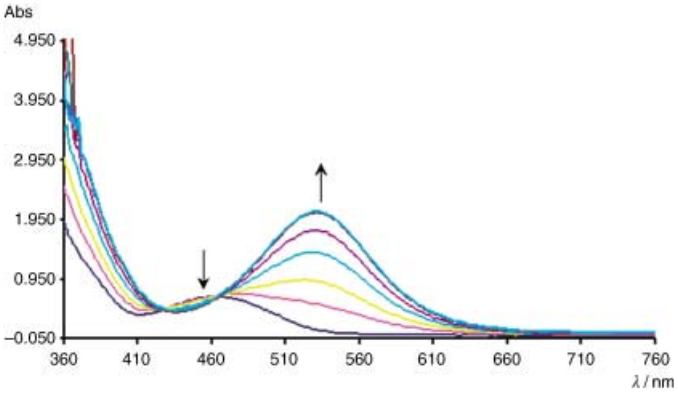

Figure 5. UV-visible spectra of the titration of alcohol **2** with 1 equivalent of $Mg(ClO_4)_2$ in CH_2Cl_2 ($c = 5\times10^{-4}$ mol dm^{-3}). The initial spectrum is that of alcohol **2** and the final spectrum corresponds to the complexed form. Arrows indicate the absorptions that increased (up) and decreased (down) during the experiment.

orange (neutral proligand) to deep purple (complexed ligand). This colour change can be used for "naked-eye" detection of Mg^{2+}, even in the presence of Ca^{2+}. The HE band is also red-shifted, although only very little.

The bathochromic shift of the LE band and the remarkable increase in its molar absorptivity are consistent with an increase in the electronic interaction in the resulting complex, as the complexation process through the C=N–C group implies a lowering of the energy gap between the d_π orbitals of the iron atom (HOMO) and the π* orbital of the acceptor group (LUMO). This observation agrees with the appearance of an irreversible reduction wave in the CV of the complexed form of **2**, which is not observed for the proligand, and might be attributed to the reduction of the now highly polarised endocyclic C=N double bond. The complexation process in which the binding site (C=N–C) interacts with the cation gives rise to a more stabilised π* orbital in the C=N group, which acts as acceptor in the MLCT process. Consequently, the oxidant character of this group is enhanced and the charge-transfer process from the ferrocenyl (which acts as the donor group) to the acceptor unit, is then favoured upon cation binding.

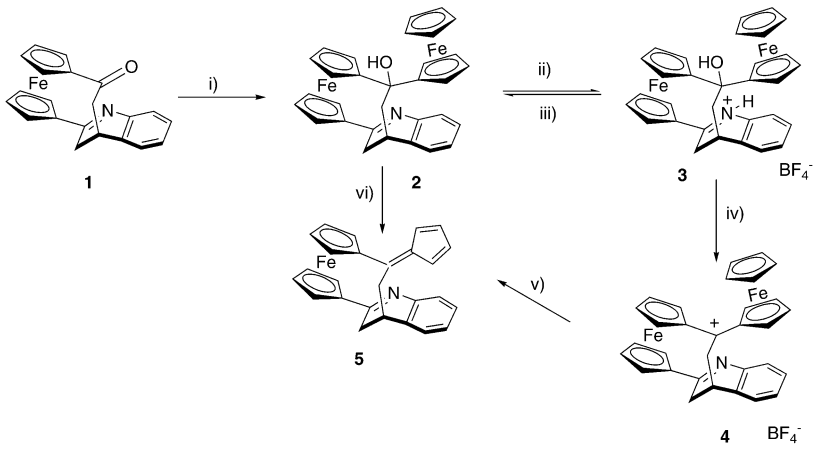

Scheme 2. Reagents and conditions: i) Fec-Li/THF, RT, 30 min, 80%; ii) 0.1 M HBF_4/CH_3CN (1 equiv); iii) K_2CO_3/MeOH, CH_3CN; iv) 0.1 M HBF_4/CH_2Cl_2 (1 equiv), 90%; v) a) 0.1 M HBF_4/CH_2Cl_2 (1 equiv) 90%; b) SiO_2, 10% Et_3N/*n*-hexane; vi) a) HCl (g)/CH_2Cl_2/$NH_4^+PF_6^-$; b) SiO_2 10% Et_3N/*n*-hexane, 90%.

The electrochemical and spectrophotometric data therefore indicate that the complexation process takes place only through the C=N−C group, with no complementary participation of the OH, a result which is consistent with the relative spatial orientation found for both groups in the solid state (X-ray structure of **2**) and in solution (NOE experiments of **2**). The association constant of the **2**·Mg^{2+} complex ($K_a = 1.8\times10^8\,M^{-2}$) could be evaluated by means of a UV-visible spectrophotometric titration.[33] Two well-defined isosbestic points were found at 428 and 464 nm (Figure 5), indicating that a neat interconversion between complexed and uncomplexed species occurs. A Job's method experiment carried out between **2** and $Mg(ClO_4)_2$ in dichloromethane at 25 °C revealed a ML_2 stoichiometry.[34] It is important to note that the association constant determined by UV-visible spectrophotometry corresponds to the complexation of the Mg^{2+} ion by neutral **2**, whereas the voltammetric shift reflects the interaction of the guest cation with the oxidised ligand.

Protonation of **2**: When **2** was treated with one equivalent of HBF_4 in acetonitrile, the N-protonated salt **3** was isolated as a deep purple solid. This, in turn, can be deprotonated by potassium carbonate in methanol to give the starting alcohol **2**. Treatment of the salt **3** with one equivalent of HBF_4 in dichloromethane afforded the diferrocenylcarbenium salt **4**, a green solid, in 90% yield. Complex **4** is highly persistent and thermally stable in the solid state and in dichloromethane, even when exposed to air. Direct conversion of alcohol **2** into **4** was achieved by addition of two equivalents of HBF_4 in dichloromethane at room temperature. However, when this treatment was carried out in acetonitrile, a complex mixture was obtained in which neither the N-protonated salt **3** nor the diferrocenylcarbenium salt **4** could be detected.

Further addition of one equivalent of HBF_4 to a solution of **4** in dichloromethane yielded the ferrocenylfulvene derivative **5** in 90% yield. This compound can also be prepared directly from **2**, in almost quantitative yield, by the action of an excess of dry hydrogen chloride. When this conversion was carried out in the presence of ammonium hexafluorophosphate, the reaction rate was increased. We have also found that compound **4** is slowly transformed into **5**, although in moderate yield, in acetonitrile at room temperature (Scheme 2).

In order to gain an insight of the stepwise protonation of **2**, spectrophotometric and electrochemical studies were performed. A solution of the compound **2** in dichloromethane was titrated with HBF_4 in dichloromethane and the absorption spectra were taken after each addition. The evolution of the UV-visible spectra is shown in the Supporting Information (Figure II). Upon addition of sub-stoichiometric quantities of HBF_4, the two characteristic charge-transfer absorption bands of ferrocenyl derivatives underwent a red-shift with an intensity increase, as predicted by the theoretical model III, developed by Marder et al.,[32] since both transitions involve charge transfer to the same empty acceptor-based orbital. As expected from its higher energy, the HE band ($\varepsilon = 10244\,M^{-1}cm^{-1}$) experienced a smaller red-shift (23 nm) than the LE band ($\varepsilon = 3549\,M^{-1}cm^{-1}$) (66 nm). These changes are observed until one equivalent of acid is added. After addition of the second equivalent of acid, the spectrum of the resulting diferrocenylcarbenium salt **4** is very different from its precursor. The resulting HE band and the first LE band are almost identical to those found in the neutral alcohol **2**. This addition also induces the appearance and development of a new broad band in the visible region at 641 nm ($\varepsilon = 3084\,M^{-1}cm^{-1}$). This explains the dark green colour of **4** and might be ascribed to a relevant transition to the iron-centred orbitals with the empty p orbital of the α-carbocationic centre.[35] The observation of some well-resolved isosbestic points during the protonation of **2** (at 320, 428 and 464 nm) and of **3** (at 245, 507, and 565 nm) indicates that there is no decomposition.

The electrochemical behaviour of compound **2** in the presence of variable concentrations of HBF_4·Et_2O was also investigated by CV in order to obtain further details about the protonation process. Thus, upon addition of sub-stoichiometric amounts of HBF_4 to a solution of **2** in dichloromethane, clear evolution of the second wave from $E_{1/2} = 0.740$ V to $E_{1/2} = 1.060$ V ($\Delta E_{1/2} = 320$ mV), and the appearance of a new irreversible reduction wave at $E_{1/2} = -0.560$ V, were observed (Figure 6). Maximum perturbation of the CV was obtained with two equivalents of added acid and, at this point, the second wave disappears. Interestingly, the new anodic wave has a typical diffusional shape, while, in contrast, a sharp cathodic stripping peak was observed. This indicates the precipitation of the oxidised protonated salt onto the electrode upon oxidation; on the reverse scan it redis-

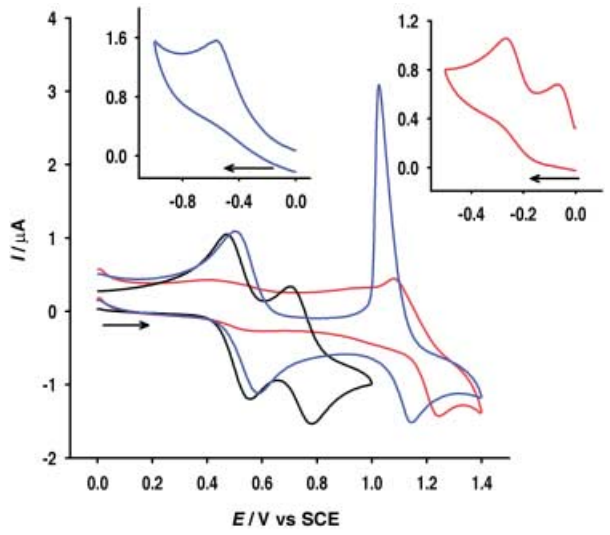

Figure 6. Voltammetric response of compound **2** (1 mM) in CH_2Cl_2 before (black) and after addition of 2 equivalents of HBF_4 (blue), and after addition of 4 equivalents of HBF_4 (red). Scan rate: 0.2 V s^{-1}. Upper inset reductive scan (0.2 V s^{-1}): left for **3** and right for **4**.

solves as it is reduced. If a small amount of acetonitrile is added to the dichloromethane electrolyte medium, the cathodic stripping peak disappears. The value of the redox potential shift on protonation ($\Delta E_{1/2} = 320$ mV) deviates by 64.6 mV from the theoretical value (255.4 mV) obtained from Plenio's relationship ($y = (-2.7 + 2.1x) \times 10^2$) between the inverse iron–nitrogen separation (x; 399.4 pm for **2**) and the shifts of the potential (y) found on protonation of several types of aza-substituted ferrocenes.[5] This deviation indicates that, apart from the electrostatic interaction between the complexed Mg^{+2} ion and the disubstituted ferrocene unit, an additional interaction between the ferrocene moieties should exist.

Further addition of two equivalents of acid produced dramatic changes in the CV. The first wave vanishes and a quasi-reversible wave at $E_{1/2} = 1.160$ V ($\Delta E_p = 140$ mV) appears. Remarkably, two well-defined irreversible reduction waves appear at -0.070 and -0.260 V versus SCE. These are attributed to the two-electron reduction of the carbenium centre. That this CV corresponds to the diferrocenylcarbenium salt **4** was confirmed by comparison with the CV of a pure sample of **4** recorded under the same conditions.

Spectroscopic characterisation of **4**: The structure of **4**, which is both a carbenium ion and a [5]ferrocenophane, has been elucidated from spectroscopic data. The high stability of carbenium ion **4** permits its accurate mass detection by high-resolution positive FAB-MS. The mass spectrum displayed an intense isotopic cluster, peaking at $m/z = 524$, assignable to the molecular ion. The relative abundance of the isotopic cluster was in good agreement with the simulated spectrum of $[M]^+$.

The room temperature 400 MHz ^{1}H NMR spectrum[36] of **4** was completely assigned (with the exception of the aromatic protons) by ^{1}H,^{1}H COSY, NOESY and spin-decoupled experiments. The diastereotopism of all the protons of the three substituted Cp rings is immediately apparent from the ^{1}H NMR spectrum of **4** (Table 1). The assignment of the protons corresponding to the different Cp rings present in the molecule, as well as the four diastereotopic protons present in the two methylene groups of this structure, were achieved by inspection of the ^{1}H,^{1}H COSY and two-dimensional NOESY spectra (Figure 3). In addition to full characterisation of these protons, some differences observed among the chemical shifts of the protons in the Cp_1, Cp_2 and Cp_3 rings are noted. In the Cp_3 ring a large deshielding for the β and β′ protons, with respect to that of the α and α′ protons, is observed ($\Delta\delta_{2'',3''} = 1.10$ and $\Delta\delta_{5'',4''} = 0.79$ ppm). This fits in with this cation having an important resonance contribution from a η^6-fulvene-η^5-cyclopentadienyliron(II) unit, with additional π-bonding of the metal with the exocyclic double bond. In this context it is also important to underline that the δ values for the β protons (H3″and H4″) are the largest observed for these type of protons in α-ferrocenylcarbenium ions.[37]

Direct metal participation in the stabilisation of the positive charge promotes significant bending of the exocyclic carbenium atom out of the Cp ring plane towards the central iron atom (Fe2). Consequently, the electronic density on the 2″- and 5″-positions have been found to be significantly increased, giving rise to a shielding of those protons with respect to H3″ and H4″, for which the opposite effect has been found.[38] These last two protons, H3″ and H4″, can be considered as fulvene-like protons. Interestingly, in the ^{1}H NMR spectrum of ferrocenylfulvene derivative **5**, the fulvene protons appear in the same region (6.4–6.7 ppm). On the other hand, the chemical shifts corresponding to the protons of the Cp_1 moiety clearly indicate that the iron atom in this ferrocene unit does not take part in stabilisation of the positive charge. The expected δ values for the β and β′ protons should thus be larger than those for the α and α′ protons.[34a] However, the observed situation is that the α and α′ protons are unshielded, with respect to the β and β′ protons ($\Delta\delta_{2,3} = -0.14$ and $\Delta\delta_{5,4} = -0.83$), following the typical pattern of a ferrocene unit linked to an electron-withdrawing group.[39]

Finally, the pattern observed for the δ values of the protons in the Cp_2 ring are in accordance with those observed in ferrocene rings monosubstitued with an electron withdrawing group: $\delta H2' > \delta H5' > \delta H3' > \delta H4'$ ($\Delta\delta_{5',4'} = -0.54$ and $\Delta\delta_{2',3'} = -0.35$). This parallels the observed pattern in the structurally related Cp_2 in alcohol **2**.

^{57}Fe Mössbauer spectroscopy has been employed to probe the iron environments in the prepared compounds (Table 4). At 77 K the neutral alcohol **2** shows one quadrupole split doublet of narrow linewidth with an isomer shift (IS) and quadrupole splitting (QS) in the normal range for ferrocenes.[40] There is no differentiation of the iron atoms, as shown by Mössbauer. The N-protonated salt **3** exhibits two nested quadrupole split doublets of equal relative intensity. The smallest of the QS values is lower than that for the parent alcohol **2**. This is expected as protonation increases the electron-withdrawing character of the C=N double bond and now favours backbonding from the ε_2 ($d_{x^2-y^2}$, d_{xy}) iron-

Table 4. ^{57}Fe Mössbauer parameters.

Compound	T [K]	IS	QS	HWHM[a]
2	77	0.52	2.33	0.13
3	77	0.50	2.41	0.13
		0.50	2.09	0.15
4	77	0.50	2.51	0.13
		0.51	2.11	0.14
	300	0.43	2.50	0.11
		0.44	2.14	0.13
6	77	0.51	2.22	0.17
	300	0.44	2.20	0.14

HWHM = half width at half maximum.

based orbitals to the ring, with a consequent decrease in QS values.[41]

The diferrocenylcarbenium **4** exhibits, at both 77 K and 300 K, two overlapping quadrupole split doublets of equal relative intensity. The i.s. moves with temperature as expected and the q.s. values are independent of temperature. The i.s. is also typical of ferrocene derivatives.[43] The smaller of the q.s. values of **4** is similar to that reported for diferrocenylmethylium tetrafluoroborate (2.10 mm s^{-1} at 298 K)[42] and is lower than that for the parent alcohol **2**. The other doublet of **4** has a QS that is higher than that of **2** and is similar to those found for a series of α-ferrocenylcarbenium ions.[43] It has been postulated that high QS values (greater than that of ferrocene itself) in α-ferrocenylcarbenium systems are due mainly to the interactions between the empty p orbital on C_{exo} with several occupied metal orbitals, probably most efficiently with one lobe of the $d_{x^2-y^2}$, the central belt of d_{z^2}, or one lobe of d_{zx}. Such an interaction would disrupt the normal binding of the ferrocene system,[44] giving rise to a ring tilt angle on the ferrocene moiety and causing the d_{z^2} to take part in the bonding.[45] As a consequence, this would promote bending towards the iron centre. Values of about 2.6–2.7 mm s^{-1} represent maximal iron participation for such systems, whereas lower QS values are due to electron withdrawal through ring-based orbitals ε_1.[43]

The reported parameters are consistent with the two iron atoms having different partial charges. However, **4** can not be described as mixed-valence as, in this case, a larger difference between QS values would be expected (e.g., in mixed-valence biferrocenium derivatives, the difference between the QS values of Fe^{II} and Fe^{III} is more than 0.66 mm s^{-1}).[46]

The useful combination of ^{1}H NMR and ^{57}Fe Mössbauer spectroscopic data of the diferrocenylcarbenium ion **4** strongly suggests two different processes for stabilisation of the α-carbocationic centre. The monosubstituted ferrocene group can clearly be considered as η^6-fulvene-η^5-cyclopentadienyliron(II) (deshielding for β protons with respect to α protons) with iron participation (high QS value), whereas the disubstituted ferrocene group is acting only through cyclopentadienyl-based orbitals (deshielding for α protons with respect to β protons) without iron participation (low QS value). That the nature of diferrocenylcarbenium ion **4** as a pentafulvene complex is more than just formal is demonstrated by its easy conversion to **5**, either spontaneously or under acidic conditions. Compound **4** represents an attractive example in which two ferrocene groups linked to an α-carbocationic centre show different spectroscopic (both ^{1}H NMR and ^{57}Fe Mössbauer) characteristics.

Mixed-valence compound 6

Synthesis: Mixed-valence compound **6** was isolated in 60% yield, as a stable purple solid, by controlled oxidation of **2** with silver trifluoromethanesulfonate. When **6** was treated with an excess of 4-dimethylaminopyridine in toluene at room temperature, the alcohol **2** was obtained, in 70% yield, after chromatographic separation on a deactivated silica gel column (Scheme 3).

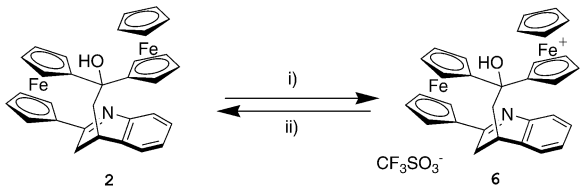

Scheme 3. Reagents and conditions: i) $AgCF_3SO_3$, toluene, RT, 1.5 h, 60%; ii) a) DMAP (excess); b) deactivated silica gel (10% ET_3N in *n*-hexane), 70%.

Physicochemical properties: A chronoamperometric study (see Figure IV in the Supporting Information) revealed the nature and purity of compound **6**. Plotting the sample current, at a fixed time of 800 ms versus the potential gave a sampled-current voltammogram, which displays two waves in the anodic and cathodic region, respectively, with the same wave height (Fe^{III}/Fe^{II} ratio 1:1). In contrast, the recorded sampled-current voltammogram for the neutral precursor **2** displayed two waves in the anodic region.

The CV of **6** in acetonitrile does not correspond to the expected one, that is, one with two reversible one-electron redox waves at +0.450 V and +0.670 V; however, it is almost identical to that obtained by complexation with $Mg(ClO_4)_2$. At the same time the CV of **6** is also very similar to the spectrum obtained by protonation of the neutral precursor **2** with one equivalent of acid, in that it displays an irreversible reduction wave at −0.450 V and two one-electron oxidation waves at +0.470 V and +1.010 V (See Figure V in the supporting information), respectively. These electrochemical results strongly suggest that, in acetonitrile, the asymmetric mixed-valence complex $\mathbf{2}^+$ exhibits an intramolecular complexation of the Fe^{III} atom by the nitrogen atom of the C=N double bond (Scheme 4). Support for this intra-

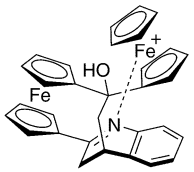

Scheme 4. Schematic representation of the intramolecular interaction in the mixed-valence complex $\mathbf{2}^+$.

molecular interaction is provided by the appearance of an absorption band at 520 nm (see Table 3) that resembles the HE band shown by $\mathbf{2}\cdot\mathbf{Mg}^{2+}$.

The mixed-valence compound **6** exhibits, both at 77 K and 300 K, a quadrupole split doublet with a QS of about 2.2 mm s^{-1}. The IS values move, as expected, with temperature and the QS values are independent of temperature. The observed quadrupole split doublet, even at 77 K, is associated with a mixed-valence state in which the intramolecular electron-transfer rate is greater than the Mössbauer timescale (10^7 s^{-1}) (Table 4). In **6** the QS is larger than those observed for other valence-delocalised biferrocenium cations. In general, ferrocenyl groups (electronic ground state $^1A_{1g}$) give spectra characterised by a large QS in the range 2.0–2.2 mm s^{-1}, while the spectra of ferrocenium cations (electronic ground state $^2E_{2g}$) are characterised by a small or vanishing QS. In localised mixed-valence biferrocenium cations, the value of the QS in the ferrocenyl moiety is slightly smaller than that expected for an Fe^{II} ferrocenyl unit and the Fe^{III} ferrocenium moiety has a slightly larger QS value. For asymmetric biferrocenophane mixed-valence compounds Mössbauer studies clearly indicate that the electronic ground state of the Fe^{III} unit is not pure $^2E_{2g}$ and larger QS values are observed. In these compounds, the Cp rings are tilted from the parallel geometry of ferrocenium. Bending back the Cp rings leads to an increase of $d_{x^2-y^2}$,d_{xy}-ring overlap and the metal nonbonding orbitals start to interact with the ligand π orbitals. Under these circumstances the iron ion loses some of its Fe^{III} character and there is consequently an increase in the QS value. In addition, an intramolecular interaction between the Fe^{III} atom and the nitrogen atom of the ferrocenophane framework (as evidenced by CV) also contributes to this increased QS.

IR spectroscopy has often been used to evaluate the rate of electron-transfer in mixed-valence compounds in the solid state when a suitable vibrator is available on one of the metallic termini. In these cases, when the electron-transfer is faster than the timescale (10^{13} s^{-1}), an averaging of this specific vibrational mode is observed for the mixed-valence compound **6** relative to the neutral compound **2** and the dioxidised $\mathbf{2}^{2+}$ species. A spectrum corresponding to the overlap of both spectra is obtained in the opposite case; that is, when a slow electron-transfer process takes place.[7,47]

Previous work on mixed-valence biferrocenes indicates that the perpendicular C–H bending band is the best indicator of the iron oxidation state. This band is seen at 815 cm^{-1} for neutral ferrocene and at 850 cm^{-1} for ferrocenium salts. A localised mixed-valence biferrocenium cation should exhibit one C–H bending band for the Fe^{II} ferrocenyl moiety and another one for the Fe^{III} ferrocenium moiety,[46d,48] while only one averaged band is expected for delocalised mixed-valence species. In our case, the IR spectrum of the neutral form **2** displays a C–H bending vibration band at 818 cm^{-1}, while in the diferrocenylcarbenium salt **4** this band appears at 843 cm^{-1}.

The IR spectra of the N-protonated salt **3** and the mixed-valence compound **6** only show one C–H bending vibration at 835 cm^{-1}. These findings are in agreement with the electrochemical results that indicate a partial positive polarisation of the C=N double bond induced by a through-space interaction with the Fe^{III} atom. They also point towards a fast electron-transfer process, in the solid state, for **6**.

The generation of the mixed-valence species from **2** was also performed electrochemically and monitored by UV-visible/near-IR spectroscopy. A stepwise Coulometric titration was performed on a solution of **2** in CH_2Cl_2 (3.5×10^{-3} mol L^{-1}), with $[N\mathit{n}Bu_4]PF_6$ (0.1 M) as supporting electrolyte. UV-visible/near-IR absorption spectra were regularly recorded by transferring a small aliquot of the solution contained in the electrochemical cell, for different average number of electrons (n) removed ($0\le n\le 2$), into a UV quartz cell . The UV-visible/near-IR data are collected in Table 3. Figure 7 shows the evolution of these spectra. The increase in the characteristics bands of ferrocenium ions at 520 and 630 nm is clearly observed, with a remarkable increase of the ε value for the 520 nm band when the second ferrocenium ion is formed, on transfer of more than one electron per mol.

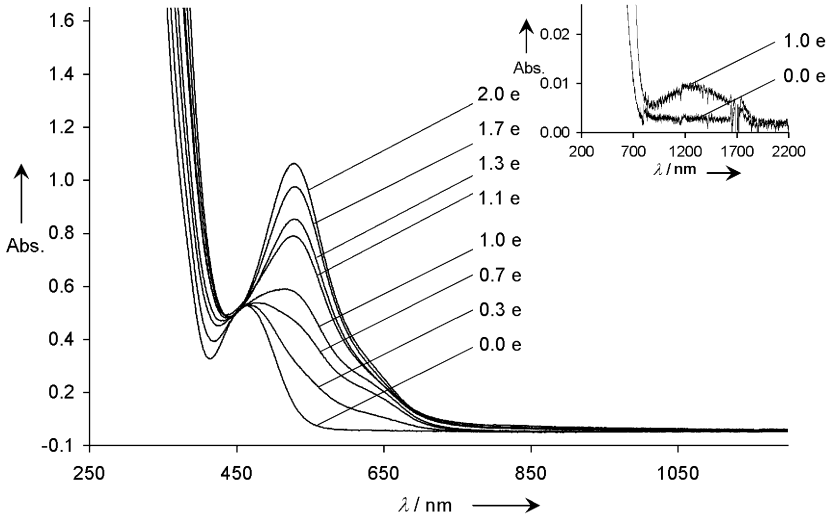

Figure 7. Evolution of the UV-Visible spectrum during the course of the oxidation of compound **2**. The average number of removed electrons is given on each spectrum. Inset: maximum of the intervalence charge-transfer band.

Interestingly, during the oxidation process of compound **2**, a new weak and broad band, centred at 1240 nm, appears. This band increases continuously until complete formation of $\mathbf{2}^{+}$ (see inset of Figure 7). The intensity of this band sub-

sequently decreases until it disappears when the dication $\mathbf{2}^{2+}$ is completely formed. This behaviour is typical of an intervalence charge-transfer (IVCT) band due to the presence of an intramolecular electron-transfer process in a class II mixed-valence compound.[7] From the characteristics of the IVCT band, the effective electronic coupling V_{ab} (in cm^{-1}) between both ferrocene redox centres can be determined, by using Equation (1) developed by Hush.[49]

$$V_{ab} = [2.05 \times 10^{-2} \sqrt{\varepsilon_{max} \nu_{max} \Delta\nu_{1/2}}] R^{-1} \quad (1)$$

In this equation $\Delta\nu_{1/2}$ (in cm^{-1}) is the half-height band width of the IVCT band, R (in Å) is the distance between the redox centres (in this case the intermetallic distance, as determined by the X-ray structure, has been used), ε_{max} (in $M^{-1}cm^{-1}$) is the maximum molar extinction coefficient, and ν_{max} (in cm^{-1}) is the wavenumber at the maximal absorbance. Equation (1) gives an effective electronic coupling (V_{ab}) for $\mathbf{2}^{+}$ of 90 cm^{-1} (0.0112 eV), which represents a weak coupling between the two ferrocene units, since it is only half the value observed in a diferrocene system linked by a long chain of six ethylene bonds.[50]

Unfortunately, the strong resemblance between the absorption spectra of $\mathbf{2{\cdot}Mg}^{2+}$ and the mixed-valence species $\mathbf{2}^{+}$ has prevented a detailed study of the electrochemically induced switchable chemosensor properties of **2**.

Conclusion

Diferrocene derivative **2**, which incorporates an aza-substituted bridge and has a ferrocenophane architecture with a ferrocenyl susbtituent, functions as a highly selective chemosensor for Mg^{2+} ions, while not showing any response to Ca^{2+} or alkaline ions. The response of **2** to Mg^{2+} can be detected either by electrochemical or optical techniques, even in the presence of other metal ions. The presence of two redox moieties in compound **2** allows formation of the mixed-valence compound, which, interestingly, shows moderate electronic coupling between both ferrocene units. It is therefore a new class II mixed-valence system in which intramolecular electron transfer has been studied by different spectroscopic techniques.

The reported properties of this new multifunctional ion-sensing derivative demonstrate that, with proper design, more efficient switchable chemosensors could be developed in the future.

Experimental Section

General methods: All reactions were carried out under N_2 and with solvents that were dried by routine procedures. All melting points were determined on a Kofler hot-plate melting point apparatus and are uncorrected. IR spectra were determined as Nujol emulsions or films on a Nicolet Impact 400 spectrophotometer. ^1H and ^{13}C NMR spectra were recorded on a Bruker AC200, 300 or 400 MHz instrument, and chemical shifts are referenced to signals of tetramethylsilane. Mössbauer spectra, obtained on an ES-Technology MS-105 spectrometer with a 100 MBq ^{57}Co source in a rhodium matrix at ambient temperature, were referenced to natural iron at 298 K. Solid samples were prepared by grinding with boron nitride. Parameters were obtained by fitting the data with Lorentzian lines, errors $< \pm 0.01$ mm s^{-1}. The EI and FAB^+ mass spectra were recorded on a Fisons AUTOSPEC 500 VG spectrometer, with 3-nitrobenzyl alcohol as a matrix. Microanalyses were performed on a Perkin–Elmer 240C instrument. Electrochemical measurements were taken with a QUICELTRON potentiostat/galvanostat controlled by a personal computer and driven by dedicated software. Electrochemical experiments were conducted in a conventional three-electrode cell, under a nitrogen atmosphere, at 25 °C. The working electrode was a Pt disk (1 mm in diameter), polished before each recording. The auxiliary electrode was a platinum wire. The reference electrode was SCE. All potentials are quoted with respect to SCE, except where noted. The experiments were in acetonitrile or dichloromethane solutions containing 0.1 M $[NnBu_4]ClO_4$ (**WARNING**:**CAUTION**) as supporting electrolyte. Under these experimental conditions, the ferrocenium/ferrocene couple was observed at +0.405 V versus SCE in acetonitrile and at +0.535 V versus SCE in dichloromethane. Deoxygenation of the solutions was achieved by bubbling with nitrogen for at least 10 minutes. Cyclic voltammetry (CV) curves were recorded at scan rates of 0.050–1 V s^{-1} and the scan potential was obtained in both positive and negative directions. The differential pulse voltammtery (DPV) curves were recorded at a 4 mV s^{-1} scan rate with a pulse height of 10 mV and a step time of 50 ms.

1,1′-[(3,4-Dihydro-2,4-quinolinediyl)(2-ferrocenyl-2-hydroxy-1,2-ethanediyl)]ferrocene (2): A solution of ferrocenyllithium, preparared by reaction of ferrocene (0.5 g, 2.68 mmol) and *t*BuLi (1.33 mL of a 1.7 M pentane solution, 2.26 mmol) in dry THF (5 mL) at 0 °C for 1 h, was added dropwise to a solution of **1** (0.2 g, 0.56 mmol) in THF (10 mL). The solution was stirred at room temperature for 10 min, then H_2O (20 mL) was added. The reaction mixture was extracted with CH_2Cl_2 (3 × 50 mL). The combined organic layers were washed with a saturated solution of NaCl (3 × 50 mL), then dried over anhydrous Na_2SO_4 and evaporated under reduced pressure. The crude product was purified by chromatography on a previously deactivated silica gel column, with 1:1 EtOAc/*n*-hexane as eluent, to give **2** in 80 % yield as an orange solid. This was crystallised from CH_2Cl_2/*n*-hexane (1:3). M.p. 290–293 °C (decomp); elemental analysis calcd (%) for $C_{31}H_{27}Fe_2NO$ (541.3): C 68.79, H 5.03, N 2.59; found: C 68.55, H 4.88, N 2.70.

3,4-Dihydroquinolium salt 3: A stirred solution of the alcohol **2** (73 mg, 0.14 mmol), in dry CH_2Cl_2 (10 mL), was treated dropwise with 1 equiv of the appropriate acid (HBF_4 or CF_3SO_3H) (e.g., 1.4 mL of a 0.1 M solution of HBF_4 in CH_2Cl_2), during which the orange colour of the solution changed to a deep purple. The resulting mixture was stirred for 5 min at room temperature, then the solvent was removed under vacuum to give a deep purple residue which was triturated with diethyl ether (10 mL). The purple solid that formed was isolated in almost quantitative yield and recrystallised by slow diffusion of Et_2O into a dilute solution of the compound in CH_2Cl_2. **3a** (X = BF_4): M.p. 222–225 °C (decomp); **3b** (X = CF_3SO_3): M.p. 215–220 °C (decomp).

Diferrocenylcarbenium 4: A stirred solution of the alcohol **2** (73 mg, 0.14 mmol) in dry CH_2Cl_2 (10 mL) was treated dropwise with 2 equiv of HBF_4 (2 × 1.4 mL of a 0.1 M solution of HBF_4 in CH_2Cl_2). During the addition, the orange colour of the solution evolved to a deep purple colour and finally to the green colour of the carbenium species. After the addition, the solution was stirred for 5 min, then the solvent was removed in vacuo. The crude product was treated with acetone/CH_2Cl_2 (1:3) and the resulting powder was washed with CH_2Cl_2 (4 × 2 mL) to give a deep green product, in 90 % yield. This was crystallised by slow diffusion of CH_2Cl_2 into a dilute solution of the compound in acetone. M.p. > 300 °C; FAB^+-HRMS: calcd for $C_{31}H_{26}NFe_2$: 524.0760; found: *m*/*z* (%): 522.0809 (15), 524.0765 (100), 525.0801 (79).

1,1′-[(3,4-Dihydro-2,4-quinolinediyl)(2-cyclopentadienylidene-1,2-ethanediyl)]ferrocene (5):

Method A: A 0.1 M solution of $[NBu_4]PF_6$ in dry CH_2Cl_2 (10 mL) was treated with a solution of **2** (0.2 g, 0.37 mmol) in dry CH_2Cl_2 (5 mL), and the reaction mixture was stirred for 5 min at room temperature. A stream of dry HCl was bubbled through the mixture for 1 h, during which a clear evolution of the colour of the solution, from orange to purple to green to purple, was observed. When the deep purple colour was persistent, the reaction mixture was filtered through a deactivated

(10% Et_3N in *n*-hexane) silica gel layer. The filtrate was evaporated to dryness and purified by chromatography on a deactivated silica gel column, using EtOAc/*n*-hexane (9:1) as eluent, to give **5**, in almost quantitative yield, as a red solid. This was crystallised by slow diffusion of *n*-hexane into a diluted solution of the compound in CH_2Cl_2.

Method B: A solution of the diferrocenylcarbenium **4** (0.1 g, 0.16 mmol) in CH_2Cl_2 (10 mL) was treated with HBF_4 (1 equiv., 1.1 mL of a 0.1 M solution of HBF_4 in CH_2Cl_2) and the mixture was stirred at room temperature and under nitrogen for 30 min, during which the deep green colour of the solution changed to deep purple. A crystalline sample in 90% yield was obtained following the same procedure as described above.

Method C: A solution of the diferrocenylcarbenium **4** (0.1 g, 0.16 mmol) in CH_3CN (10 mL) was stirred at room temperature for 10 min to give a black precipitate, which was filtered off. The filtrate was evaporated to dryness and the product was isolated, as described above, in 90% yield. M.p. 167–170°C; elemental analysis calcd (%) for $C_{26}H_{21}FeN$ (403.3): C 77.43, H 5.25, N, 3.47; found: C 77.14, H 5.30, N 3.27.

Mixed-valence compound 6: A sample of this mixed-valence compound was prepared by adding a solution of $AgCF_3SO_3$ (0.024 g, 0.094 mmol) in dry toluene (10 mL) to a solution of the alcohol **2** (0.051 g, 0.094 mmol) in the same solvent (50 mL). The reaction mixture was stirred at room temperature and under nitrogen for 1.5 h. The dark brown microcrystals formed were collected by filtration and washed with three portions of toluene (3×10 mL). The solid was dissolved in $CHCl_3$ (25 mL) and stirred at room temperature and under nitrogen for 10 min to give a deep purple solution and a dark precipitate. The solution was filtered under nitrogen and the precipitate was washed with $CHCl_3$ (3×10 mL). The combined organic layers were evaporated to dryness under reduced pressure. The resulting residue was triturated with dry Et_2O to give **9** as a deep purple solid in 60% yield. This was crystallised from CH_2Cl_2/toluene (1:1). M.p: 227–230°C (decomp); IR (CH_2Cl_2): $\tilde{\nu}$=3468, 1642, 1618, 1574, 1287, 1263, 1169, 1038, 835, 758 cm^{-1}; MS (FAB$^+$): *m*/*z* (%): 691 (5) [M^++1], 542 (100) [M^++1−CF_3SO_3]; elemental analysis calcd (%) for $C_{32}H_{28}F_3Fe_2NO_4S$ (691.3): C 55.60, H 4.08, N2.03; found: C 55.42, H 4.28, N 1.95.

X-ray crystal structure analysis:

Data collection: A Nonius Kappa CCD with an area detector was used. 19153 reflections were measured by means of ϕ- and ω-scans and extracted from the frames (DENZO-SMN).

Structure solution and refinement: Non-hydrogen atoms were refined anisotropically on F^2 (SHELXL 97), hydrogen atoms of the carbon atoms were refined at calculated positions, the hydrogen atom of the hydroxyl group was refined with an isotropic displacement parameter; *R* values for 320 parameters and 2402 observed reflections [$I>2\sigma(I)$]: R_1=0.0418 and wR_2=0.0977.

Crystal data: $C_{31}H_{27}Fe_2NO$, monoclinic, space group $P2_1/n$, a=11.3545(4), b=10.8175(6), c=18.725(1) Å, β=92.667(3)°, V=2297.45(19) Å^3, Z=4, T=233(2) K, $\lambda(Mo_{K\alpha})$=0.71073 Å, $F(000)$=1120, μ=1.289 mm^{-1}, ρ_{calcd}=1.565 gcm^{-3}, yellow prism 0.4×0.1×0.05 mm. CCDC-215840 contains the supplementary crystallographic data for this paper. These data can be obtained free of charge via www.ccdc.cam.ac.uk/conts/retrieving.html (or from the Cambridge Crystallographic Data Centre, 12 Union Road, Cambridge CB2 1EZ, UK; fax: (+44) 1223–336–033; or e-mail: deposit@ccdc.cam.uk).

Acknowledgement

We gratefully acknowledge the financial support of the DGI (Ministerio de Ciencia y Tecnología, Spain) (Projects. BQU2001-0014 and MAT2000-1388-C03-01), Fundación Séneca (CARM) (Project. No. PB/72/FS/02) and DGR Catalunya (Project 2001 SGR00362). We also wish to thank Prof. P. Deyá, Dr. A. Frontera and C.Garau (UIB) for computational facilities and helpful suggestions. The Biotechnology and Biological Sciences Research Council (UK) are thanked for funding (D.J.E.). J.L.L. and V.L., who is enrolled in the Ph.D. programme of the UAB (Universitat Autónoma de Barcelona), thank the MCyT (Spain) for their studentships.

[1] *Ferrocenes, Homogeneous Catalysis, Organic Synthesis, Material Science* (Eds.: A. Togni, T. Hayashi), VCH, Weinheim **1995**.

[2] a) G. W. Gokel, *Chem. Soc. Rev.* **1992**, *21*, 39–46; b) P. D. Beer, *Adv. Inorg. Chem.* **1992**, *39*, 79–157; c) P. L. Boulas, M. Gomez-Kaifer, L. Echegoyen, *Angew. Chem.* **1998**, *110*, 226–258; *Angew. Chem. Int. Ed.* **1998**, *37*, 216–247; d) P. D. Beer, P. A. Gale, G. Z. Chen, *Coord. Chem. Rev.* **1999**, *185/186*, 3–36; e) P. D. Beer, P. A. Gale, *Adv. Phys. Org. Chem.* **1998**, *31*, 1–90; d) P. D. Beer, P. A. Gale, *Angew. Chem.* **2001**, *113*, 502–532; *Angew. Chem. Int. Ed.* **2001**, *40*, 486–516.

[3] a) J. C. Medina, T. T. Goodnow, M. T. Rojas, J. L. Atwood, B. C. Lynn, A. E. Kaifer, G. W. Gokel, *J. Am. Chem. Soc.* **1992**, *114*, 10583–10595; b) P. D. Beer, Z. Cheng, M. G. B. Drew, J. Kingston, M. Ogden, P. Spencer, *J. Chem. Soc. Chem. Commun.* **1993**, 1046–1048; c) H. Plenio, H. El-Desoky, J. Heinze, *Chem. Ber.* **1993**, *126*, 2403–2408; d) M. J. L. Tendero, A. Benito, R. Martínez-Mañez, J. Soto, J. Payá, A. J. Edward, P. R. Raithby, *J. Chem. Soc. Dalton Trans.* **1996**, 343–352; e) H. Plenio, C. Aberle, *Organometallics* **1997**, *16*, 5950–5957; f) H. Plenio, C. Aberle, *Angew. Chem.* **1998**, *110*, 1467–1470; *Angew. Chem. Int. Ed.* **1998**, *37*, 1397–1399; g) M. E. Padilla-Tosta, R. Martínez-Mañez, T. Pardo, J. Soto, M. J. L. Tendero, *Chem. Commun.* **1997**, 887–888; h) H. Plenio, C. Aberle, Y. Al-Shihaded, J. M. Lloris, R. Martínez-Mañez, T. Pardo, J. Soto, *Chem. Eur. J.* **2001**, *7*, 2848–2861.

[4] P. D. Beer, P. A. Gale, G. Z. Chen, *J. Chem. Soc. Dalton Trans.* **1999**, 1897–1909.

[5] H. Plenio, J. Yang, R. Diodone, J. Heinze, *Inorg. Chem.* **1994**, *33*, 4098–4104.

[6] S. R. Miller, D. A. Gustowski, Z. H. Chen, G. W. Gokel, L. Echegoyen, A. E. Kaifer, *Anal. Chem.* **1988**, *60*, 2021–2024.

[7] M. Robin, P. Day, *Adv. Inorg. Chem. Radiochem.* **1967**, *10*, 247–422.

[8] a) D. Astruc, *Electron Transfer and Radical Processes in Transition-Metal Chemistry*, VCH, New York, **1995**; b) "Electron Transfer in Inorganic, Organic and Biological Systems": *Adv. Chem. Ser.* **1991**, *228*, whole volume.

[9] For reviews see: a) S. Barlow, D. O'Hare, *Chem. Rev.* **1997**, *97*, 637–669; b) D. Astruc, *Acc. Chem. Res.* **1997**, *30*, 383–391; c) J. P. Launay, *Chem. Soc. Rev.* **2001**, *30*, 386–397; d) P. Nguyen, P. Gomez-Elipe, I. Manners, *Chem. Rev.* **1999**, *99*, 1515–1548; e) W. Kaim, A. Klein, M. Glöckle, *Acc. Chem. Res.* **2000**, *33*, 755–763; f) K. D. Demadis, C. M. Hartshorn, T. J. Meyer, *Chem. Rev.* **2001**, *101*, 2655–2685.

[10] a) R. J. Crutchley, *Prog. Inorg. Chem.* **1994**, *41*, 273–325; b) C. Creutz, *Prog. Inorg. Chem.* **1983**, *30*, 1–71.

[11] a) D. E. Richardson, H. Taube, *Coord. Chem. Rev.* **1984**, *60*, 107–129; b) D. E. Richardson, H. Taube, *Inorg. Chem.* **1981**, *20*, 1278–1285; c) J. E. Sutton, H. Taube, *Inorg. Chem.* **1981**, *20*, 3125–3134; d) R. de la Rosa, P. J. Chang, F. Salaymeh, J. C. Curtis, *Inorg. Chem.* **1985**, *24*, 4229–4231; e) Y. Dong, J. T. Hupp, *Inorg. Chem.* **1992**, *31*, 3170–3172.

[12] a) W. H. Morrison, Jr., D. N. Hendrickson, *Inorg. Chem.* **1975**, *14*, 2331–2346; b) R. J. Webb, P. M. Hagen, R. J. Wittebort, M. Sorai, *Inorg. Chem.* **1992**, *31*, 1791–1801; c) S. Rittinger, D. Buchholz, M. H. Delville-Desbois, J. Linares, F. Varret, R. Boese, L. Zsolnai, G. Huttner, D. Astruc, *Organometallics*, **1992**, *11*, 1454–1456; d) P. Hudeczeck, F. H. Köhler, *Organometallics* **1992**, *11*, 1773–1775; e) T.-Y. Dong, T.-Y. Lee, S.-H. Lee, G.-H. Lee, S.-M. Peng, *Organometallics* **1994**, *13*, 2337–2348; f) T.-Y. Dong, C.-H. Huang, C.-K. Chang, H.-C. Hsieh, S.-M. Peng, G.-H. Lee, *Organometallics* **1995**, *14*, 1776–1785; g) S. Barlow, V. J. Murphy, J. S. O. Evans, D. O'Hare, *Organometallics* **1995**, *14*, 3461–3474; h) T.-Y. Dong, C.-K. Chang, S.-H. Lee, L.-L. Lai, M. Y.-N. Chiang, K.-J. Lin, *Organometallics* **1997**, *16*, 5816–5825; i) H. Hilbig, P. Hudeczek, F. H. Köhler, X. Xie, P. Bergerat, O. Kahn, *Inorg. Chem.* **1998**, *37*, 4246–4257; j) R. W. Meo, F. B. Somoza, T. R. Lee, *J. Am. Chem. Soc.* **1998**, *120*, 1621–1622; k) O. M. Heilg, M. A. Herker, W. Hiller, F. H. Köhler, A. Schell, *J. Organomet. Chem.* **1999**, *574*, 94–98.

[13] a) K. R. J. Thomas, J. T. Lin, Y. S. Wen, *J. Organomet. Chem.* **1999**, *575*, 301–309; b) K. R. J. Thomas, J. T. Lin, K.-J. Lin, *Organometallics* **1999**, *18*, 5285–5291; c) K. R. J. Thomas, J. T. Lin, Y. S. Wen, *Organometallics* **2000**, *19*, 1008–1012; d) A. Tárraga, P. Molina, D. Curiel, M. D. Velasco, *Organometallics* **2001**, *20*, 2145–2152.

[14] a) A. Ohkubo, T. Fujita, S. Ohba, K. Aramaki, H. Nishihara, *J. Chem. Soc. Chem. Commun.* **1992**, 1553–1555; b) Y. Yamada, J. Mizutani, M. Kurihara, H. Nishihara, *J. Organomet. Chem.* **2001**, *637–639*, 80–83.
[15] L. M. Tolbert, X. Zao, Y. Ding, L. A. Bottomley, *J. Am. Chem. Soc.* **1995**, *117*, 12891–12892.
[16] a) G. Ferguson, C. Glidewell, G. Opromolla, C. M. Zakaria, P. Zanello, *J. Organomet. Chem.* **1996**, *506*, 129–137; b) G. Ferguson, C. Glidewell, G. Opromolla, C. M. Zakaria, P. Zanello, *J. Organomet. Chem.* **1996**, *517*, 183–190.
[17] a) A. Tárraga, P. Molina, J. L. López, *Tetrahedron Lett.* **2000**, *41*, 2479–2482; b) A. Tárraga, P. Molina, J. L. López, M. D. Velasco, D. Bautista, P. G. Jones, *Organometallics* **2002**, *21*, 2055–2065.
[18] See reference [12g].
[19] a) T. J. Curphey, J. O. Santer, M. Rosenblum, J. H. Richards, *J. Am. Chem. Soc.* **1960**, *82*, 5249–5250; b) T. E. Bitterwolf, A. C. Ling, *J. Organomet. Chem.* **1972**, *40*, 197–203.
[20] a) A. F. Cunningham, Jr., *J. Am. Chem. Soc.* **1991**, *113*, 4864–4870; b) A. F. Cunningham, Jr., *Organometallics* **1994**, *13*, 2480–2485; c) A. F. Cunningham, Jr., *Organometallics* **1997**, *16*, 1114–1122; d) M. J. Mayor-López, J. Weber, B. Mannfors, A. F. Cunningham, Jr., *Organometallics* **1998**, *17*, 4983–4991; e) A. Irigoras, J. M. Mercero, I. Silanes, J. M. Ugalde, *J. Am. Chem. Soc.* **2001**, *123*, 5040–5043.
[21] The process observed was reversible, according to the following criteria: 1) separation of 60 mV between cathodic and anodic peaks, 2) close-to-unity ratio of the intensities of the cathodic and anodic currents and 3) constancy of the peak potential on changing the sweep rate in the CV. The same halfwave potential values have been obtained from the DPV peaks and from an average of the cathodic and anodic cyclic voltammetric peak.
[22] F. A. Cotton, J. P. Donahue, C. Lin, C. A. Murillo, *Inorg. Chem.* **2001**, *40*, 1234–1244.
[23] Experiments used the ligand **2** (1 mM) in CH_3CN/CH_2Cl_2 (3:2) in the presence of $[NnBu_4]ClO_4$ (0.1 M) and decamethylferrocene (1 mM), used as an internal standard. The potential of the $DCMFc^+$/DCMFc redox couple is −0.05 V versus SCE under our experimental conditions and the halfwave redox potentials were referred to this. Sequential addition of aliquots of 0.1 equivalents of 10^{-2} M solutions of the appropriate salt in CH_3CN were monitored by CV.
[24] P. Bühlmann, E. Pretsch, E. Bakker, *Chem. Rev.* **1998**, *98*, 1593–1687.
[25] P. D. Beer, K. Y. Wild, *Polyhedron* **1996**, *15*, 775–780.
[26] a) A. Chesney, M. R. Bryce, A. S. Batsanov, J. A. K. Howard, L. M. Goldenberg, *Chem. Commun.* **1998**, 677–678; b) O. B. Sutcliffe, A. Chesney, M. R. Bryce, *J. Organomet. Chem.* **2001**, *637–639*, 134–138.
[27] O. B. Sutcliffe, M. R. Bryce, A. S. Batsanov, *J. Organomet. Chem.* **2002**, *656*, 211–216.
[28] U. Siemeling, B. Neumann, H.-G. Stammler, A. Salmon, *Z. Anorg. Allg. Chem.* **2002**, *628*, 2315–2320.
[29] J. D. Carr, S. J. Coles, W. W. Asan, M. B. Hursthouse, K. M. A. Malik, J. H. R. Tucker, *J. Chem. Soc. Dalton Trans.* **1999**, 57–62, and references therein.
[30] T. Farrel, T. Meyer-Friedrichsen, M. Malessa, D. Haase, W. Saak, I. Asselberghs, K. Wostyn, K. Clays, A. Persoons, J. Heck, A. R. Manning, *J. Chem. Soc. Dalton Trans.* **2001**, 29–36, and references therein.
[31] S. Barlow, H. E. Bunting, C. Ringham, J. C. Green, G. U. Bublitz, S. G. Boxer, J. W. Perry, S. R. Marder, *J. Am. Chem. Soc.* **1999**, *121*, 3715–3723.
[32] Y. S. Sohn, D. N. Hendrickson, M. B. Gray, *J. Am. Chem. Soc.* **1971**, *93*, 3603–3612.
[33] The titration experiment was conducted by adding increasing amounts of a 2×10^{-2} M solution of anhydrous $Mg(ClO_4)_2$ in dry acetonitrile to a solution of **2** in dry dichloromethane at a constant concentration of the receptor. The value of the association constant is the average of three independent titrations.
[34] We note here that the different techniques used to monitor the metal binding do not always suggest the same stoichiometry. This is a known phenomenon in related systems and arises from the different concentrations and timescales employed in the different techniques. See: a) P. D. Beer, H. Sikanyika, C. Blackburn, J. F. McAleer, *J. Organomet. Chem.* **1988**, *350*, C15–C19; b) P. D. Beer, A. D. Keefe, H. Sikayika, C. Blackburn, J. F. McAleer, *J. Chem. Soc. Dalton Trans.* **1990**, 3289–3294.
[35] M. Ausorge, K. Polborn, T. J. Müller, *Eur. J. Inorg. Chem.* **2000**, 2003–2009.
[36] Due to poor solubility, ^{13}C NMR data for compound **4** could not be obtained.
[37] a) M. Cais, J. J. Dannenberg, A. Eisenstadt, M. I. Levenberg, J. H. Richards, *Tetrahedron Lett.* **1966**, *7*, 1695–1701; b) S. Lupan, M. Kapon, M. Cais, F. H. Herbstein, *Angew. Chem.* **1972**, *84*, 1104–1106; *Angew. Chem. Int. Ed. Engl.* **1972**, *11*, 1025–1027; c) G. K. S. Prakash, H. Buchholz, V. P. Reddy, A. Meijere, G. A. Olah, *J. Am. Chem. Soc.* **1992**, *114*, 1097–1098; d) F. L. Hedberg, H. Rosenberg, *J. Am. Chem. Soc.* **1969**, *91*, 1258–1259.
[38] J. H. Richards, E. A. Hill, *J. Am. Chem. Soc.* **1959**, *81*, 3484–3485.
[39] T. E. Pickett, C. J. Richards, *Tetrahedron Lett.* **1999**, *40*, 5251–5254.
[40] R. V. Parish, in *The Organic Chemistry of Iron, Vol. 1*, (Eds.: E. A. Koerner von Gustorf, F. W. Grevels, I. Fischler), Academic Press, **1978**, pp. 175–211.
[41] a) R. M. G. Roberts, J. Silver, *J. Organomet. Chem.* **1984**, *263*, 235–241; b) L. Korecz, M. Abou, G. Ortaggi, M. Graziani, U. Belluco, K. Burger, *Inorg. Chim. Acta* **1974**, *9*, 209–211; c) J. Silver, G. R. Fern, J. R. Miller, E. Slade, M. Ahmet, A. Houlton, D. J. Evans, G. J. Leigh, *J. Organomet. Chem.* **2001**, *637–639*, 311–317; d) A. Houlton, J. R. Miller, M. R. G. Roberts, J. Silver, *J. Chem. Soc. Dalton Trans.* **1990**, 2181–2183.
[42] R. Gleiter, R. Seeger, H. Binder, E. Fluck, E. M. Cais, *Angew. Chem.* **1972**, *84*, 1107–1109; *Angew. Chem. Int. Ed. Engl.* **1972**, *11*, 1028–1030.
[43] G. Nevshvad, R. M. G. Roberts, J. Silver, *J. Organomet. Chem.* **1982**, *236*, 237–244.
[44] A. Houlton, J. R. Miller, R. M. G. Roberts, J. Silver, *J. Chem. Soc. Dalton Trans.* **1991**, 467–470.
[45] J. Silver, *J. Chem. Soc. Dalton Trans.* **1990**, 3513–3516.
[46] a) T.-Y. Dong, C.-H. Huang, C.-K. Chang, Y.-S. Wen, S.-L. Lee, J.-A. Chen, W.-Y. Yeh, A. Yeh, *J. Am. Chem. Soc.* **1993**, *115*, 6357–6368; see reference [12e]; c) T.-Y. Dong, S.-H. Lee, C.-K. Chang, H.-M. Lin, K.-J. Lin, *Organometallics* **1997**, *16*, 2773–2786; see reference [12h]; e) T.-Y. Dong, L.-S. Chang, G.-H. Lee, S.-M. Peng, *Organometallics* **2002**, *21*, 4192–4200; f) T.-Y. Dong, B.-R. Huang, S.-M. Peng, G.-H. Lee, M. Y.-N. Chiang, *J. Organomet. Chem.* **2002**, *659*, 125–132; g) T.-Y. Dong, L.-S. Chang, G.-H. Lee, S.-M. Peng, *Inorg. Chem. Commun.* **2002**, *5*, 107–111.
[47] N. S. Hush, *Prog. Inorg. Chem.* **1967**, *8*, 391–444
[48] T.-Y. Dong, D. N. Hendrickson, K. Iwai, M. J. Cohn, A. L. Rheingold, H. Sano, S. Motoyama, *J. Am. Chem. Soc.* **1985**, *107*, 7996–8008.
[49] N. S. Hush, *Coord. Chem. Rev.* **1985**, *64*, 135–157.
[50] A.-C. Ribou, J.-P. Launay, M. L. Sachtleben, H. Li, C. W. Spangler, *Inorg. Chem.* **1996**, *35*, 3735–3740.

Received: July 28, 2003
Revised: November 3, 2003 [F5394]